

Maximum Sum-Rate of MIMO Multiuser Scheduling with Linear Receivers

Raymond H. Y. Louie^{†*}, Matthew R. McKay[‡], Iain B. Collings^{*}

[†]Telecommunications Lab, School of Electrical and Information Engineering, University of Sydney, Australia

^{*}Wireless Technologies Laboratory, ICT Centre, CSIRO, Sydney, Australia

[‡]Department of Electronic and Computer Engineering,
Hong Kong University of Science and Technology, Hong Kong

Abstract

We analyze scheduling algorithms for multiuser communication systems with users having multiple antennas and linear receivers. When there is no feedback of channel information, we consider a common round robin scheduling algorithm, and derive new exact and high signal-to-noise ratio (SNR) maximum sum-rate results for the maximum ratio combining (MRC) and minimum mean squared error (MMSE) receivers. We also present new analysis of MRC, zero forcing (ZF) and MMSE receivers in the low SNR regime. When there are limited feedback capabilities in the system, we consider a common practical scheduling scheme based on signal-to-interference-and-noise ratio (SINR) feedback at the transmitter. We derive new accurate approximations for the maximum sum-rate, for the cases of MRC, ZF and MMSE receivers. We also derive maximum sum-rate scaling laws, which reveal that the maximum sum-rate of all three linear receivers converge to the same value for a large number of users, but at different rates.

Corresponding Author:

Raymond H. Y. Louie

Sch. of Elec. and Info. Engineering, University of Sydney, NSW 2006, Australia

+61-2-9372 4244 (phone) +61-2-9351 3847 (fax), rlouie@ee.usyd.edu.au

The material in this paper has been presented in part at the IEEE Global Communications Conference (GLOBE-COM), New Orleans, LA, USA, December 2008.

I. INTRODUCTION

The use of multiple-input multiple-output (MIMO) antenna systems in multiuser environments has recently gained considerable attention. Much progress has been made on characterizing the fundamental limits and developing signal processing schemes for both the multiple-access channel and broadcast channel scenarios (see, eg. [1, 2]). In this paper, we consider the broadcast channel, which embraces a large number of important application scenarios; for example, a base-station serving multiple users in a cellular environment, or a relay node serving multiple network nodes in an ad-hoc network.

For systems with perfect feedback capabilities, i.e. when complete short-term channel state information (CSI) of all of the users are available to the transmitter, it is well-known that the optimum solution for achieving the capacity is to employ dirty paper coding (DPC). However, while DPC is capacity achieving, it also has prohibitive complexity. This, coupled with the stringent and potentially overwhelming feedback requirements, render DPC unsuitable for practical implementation. Various low complexity alternatives have been employed and studied extensively (see, eg. [1, 3, 4]), however these schemes all require perfect knowledge of the CSI at the transmitter. For increasing number of users and antennas, the amount of CSI feedback becomes large, and these schemes become impractical. In addition, inaccurate CSI feedback may lead to significant performance losses [5].

In this paper, we are interested in the practical scenarios when there is limited or no feedback of CSI at the transmitter. In this case, efficient scheduling algorithms are required for coordinating transmissions to the different users. Appropriate scheduling approaches depend on the feedback capabilities between the receivers and the transmitter, and their performance can be measured in terms of the maximum sum-rate.

For systems with no feedback capabilities, an obvious and practical scheduling approach is to employ a simple round-robin scheduling algorithm; i.e. a time-division multiple access (TDMA) scheme. The maximum sum-rate in this case becomes equivalent to the maximum sum-rate of a single user MIMO system. The single user MIMO maximum sum-rate has been extensively studied for optimal receivers (see, eg. [6, 7]), and zero forcing (ZF) linear receivers (see, eg. [8, 9]). Other results include the particular case where the number of transmit antennas is less than

or equal to the number of receive antennas in the high signal-to-noise ratio (SNR) regime, for which the maximum sum-rate has been derived for ZF and minimum mean squared error (MMSE) receivers in [10, Eq. 8.54]. In this paper, we derive new exact maximum sum-rate expressions for both the maximum ratio combining (MRC) and MMSE receivers. We also derive new maximum sum-rate expressions in the high SNR regime for MMSE receivers in the case where the number of transmit antennas is greater than the number of receive antennas, and for MRC receivers in the case of arbitrary antenna configurations. We then investigate the maximum sum-rate in the low SNR regime for each of the three linear receivers.

When limited feedback is available, the scheduling algorithm can be more sophisticated. In this paper we consider the common case of systems which feed back signal-to-interference-and-noise ratios (SINRs) and use opportunistic scheduling. In particular, we examine systems where the SINR (for each user) can be measured from each transmit antenna separately, and then fed back. In the scheduling algorithm each transmit antenna sends an independent data stream to the user with the largest corresponding SINR. Of particular interest is systems employing practical linear receivers. For the specific case of ZF, previous related results have been presented in [11], where an upper bound to the asymptotic maximum sum-rate scaling law was derived, and in [8], where an exact (albeit complicated) non-asymptotic expression was derived. Moreover, for the specific case of four transmit and two receive antennas, [12] presented maximum sum-rate scaling laws for the MRC and MMSE receivers. In this paper, we generalize these prior results, by considering the maximum sum-rate for arbitrary antenna configurations, and deriving new maximum sum-rate results for MRC, ZF and MMSE receivers. We present new accurate approximations for the maximum sum-rate, and derive exact maximum sum-rate scaling laws. We show that all three linear receivers converge to the same asymptotic maximum sum-rate as the number of users grows large, however the speed of convergence is different. Our results are confirmed through comparison with Monte Carlo simulations.

Throughout this paper, we denote $E[\cdot]$ as expectation, $(\cdot)^\dagger$ as conjugate transpose, $\text{Tr}(\cdot)$ as matrix trace, \mathbf{I}_N as a $N \times N$ identity matrix and $\mathbf{0}_{N \times M}$ as a $N \times M$ zero matrix. Also, \otimes denotes Kronecker product and $\mathcal{CN}_{M,N}(\mathbf{M}, \mathbf{V})$ represents an $M \times N$ matrix-variate complex Gaussian distribution with $M \times N$ mean matrix \mathbf{M} and $MN \times MN$ covariance matrix \mathbf{V} .

II. SYSTEM MODEL

We consider a multiuser MIMO broadcast channel scenario, where a transmitter has N_t antennas while each of the K users has N_r antennas. Each antenna at the transmitter is used to independently transmit a stream of data to a particular user, as determined by the two scheduling algorithms described in the next two sections. The received vector for the i th user can be written as

$$\mathbf{y}_i = \mathbf{H}_i \mathbf{x} + \mathbf{n}_i \quad (1)$$

where $\mathbf{H}_i \sim \mathcal{CN}_{N_r, N_t}(\mathbf{0}_{N_r \times N_t}, \mathbf{I}_{N_r} \otimes \mathbf{I}_{N_t})$ is the $N_r \times N_t$ Rayleigh fading channel matrix from the transmitter to the i th user, \mathbf{x} is the $N_t \times 1$ transmit symbol vector with $\mathbb{E}[\mathbf{x}^\dagger \mathbf{x}] = P$, and $\mathbf{n}_i \sim \mathcal{CN}_{N_r, 1}(\mathbf{0}_{N_r \times 1}, N_0 \mathbf{I}_{N_r})$ is the additive white Gaussian noise vector. If we assume that the data stream for the i th user comes from the k th transmit antenna, we can write the received vector in (1) as

$$\mathbf{y}_{i,k} = \mathbf{h}_{i,k} x_k + \sum_{j=1, j \neq k}^{N_t} \mathbf{h}_{i,j} x_j + \mathbf{n}_i \quad (2)$$

where $\mathbf{h}_{i,j}$ is the j th column vector of \mathbf{H}_i and x_j is the symbol sent from the j th transmit antenna. We assume that user i perfectly estimates their own channel matrix, \mathbf{H}_i . We also assume that the total power budget is distributed equally across the different transmit antennas, such that $\mathbb{E}[|x_j|^2] = \frac{P}{N_t}$ for $j = 1, \dots, N_t$. To recover the desired symbol, we multiply the received signal by a $1 \times N_r$ received weight vector \mathbf{w}_i^\dagger , which for MRC, ZF, and MMSE linear receivers, and their resulting received SINR, are given respectively by

$$\mathbf{w}_{\text{MRC}}^\dagger = \mathbf{h}_{i,k}^\dagger \quad \Rightarrow \quad \gamma_{i,k,\text{MRC}} = \frac{\frac{\rho}{N_t} |\mathbf{h}_{i,k}^\dagger \mathbf{h}_{i,k}|^2}{\frac{\rho}{N_t} \sum_{j=1, j \neq k}^{N_t} |\mathbf{h}_{i,k}^\dagger \mathbf{h}_{i,j}|^2 + |\mathbf{h}_{i,k}^\dagger \mathbf{h}_{i,k}|}, \quad (3)$$

$$\mathbf{w}_{\text{ZF}}^\dagger = \mathbf{g}_k^\dagger \quad \Rightarrow \quad \gamma_{i,k,\text{ZF}} = \frac{\rho}{N_t \left[\mathbf{H}_i^\dagger \mathbf{H}_i \right]_{k,k}^{-1}} \quad (4)$$

and

$$\mathbf{w}_{\text{MMSE}}^\dagger = \mathbf{h}_{i,k}^\dagger \left(\mathbf{K} \mathbf{K}^\dagger \frac{\rho}{N_t} + \mathbf{I}_{N_r} \right)^{-1} \quad \Rightarrow \quad \gamma_{i,k,\text{MMSE}} = \frac{\rho}{N_t} \mathbf{h}_{i,k}^\dagger \left(\mathbf{K} \mathbf{K}^\dagger \frac{\rho}{N_t} + \mathbf{I}_{N_r} \right)^{-1} \mathbf{h}_{i,k} \quad (5)$$

where $\rho = \frac{P}{N_0}$ is the average SNR, \mathbf{g}_k^\dagger is the k th row of $(\mathbf{H}_i^\dagger \mathbf{H}_i)^{-1} \mathbf{H}_i^\dagger$, $[\mathbf{Z}]_{k,k}$ is the (k, k) th element of \mathbf{Z} and $\mathbf{K} = \mathbf{H}_i^{\{k\}}$ is the $N_r \times (N_t - 1)$ matrix with the same elements as \mathbf{H}_i but with the k th column removed. Note that throughout this paper, we require $N_r \geq N_t$ when dealing with ZF receivers, whilst we consider arbitrary antenna configurations for MRC and MMSE.

It is convenient to define the normalized SINR as follows

$$X \triangleq \frac{N_t \gamma}{\rho} \quad (6)$$

where γ is the instantaneous SINR given for MRC, ZF and MMSE in (3), (4) and (5) respectively. For the ZF and MMSE receivers, the cumulative distribution function (c.d.f.) of X for an arbitrary user is given by [8]

$$F_{X_{\text{ZF}}}(x) = 1 - e^{-x} \sum_{k=0}^{N_r - N_t} \frac{x^k}{k!} \quad (7)$$

and [13]

$$F_{X_{\text{MMSE}}}(x) = 1 - \frac{e^{-x}}{\left(1 + \frac{\rho}{N_t} x\right)^{N_t - 1}} \sum_{k=0}^{N_r - 1} \beta_k x^k \quad (8)$$

respectively, where

$$\beta_k = \left(\frac{\rho}{N_t}\right)^k \sum_{p=\max(0, k - N_t + 1)}^k \frac{\binom{N_t - 1}{k - p}}{p! \left(\frac{\rho}{N_t}\right)^p}. \quad (9)$$

For MRC, the c.d.f. of X has been previously derived in [14]. However the resulting expression is complicated, involving multiple summations over sets, and is therefore not easily amenable to further analysis. In Appendix A, we show that the SINR c.d.f. admits a simpler representation given by

$$F_{X_{\text{MRC}}}(x) = 1 - \frac{e^{-x}}{\left(1 + \frac{\rho}{N_t} x\right)^{N_t - 1}} \sum_{k=0}^{N_r - 1} \sum_{p=0}^k \frac{\alpha_{p,k} x^k}{\left(1 + \frac{\rho}{N_t} x\right)^p} \quad (10)$$

where

$$\alpha_{p,k} = \frac{\binom{N_t + p - 2}{p} \left(\frac{\rho}{N_t}\right)^p}{(k - p)!}. \quad (11)$$

The corresponding probability density functions (p.d.f.) for ZF, MMSE, and MRC are obtained

by taking the derivative of (7), (8), and (10) respectively, and are given by

$$f_{X_{\text{ZF}}}(x) = \frac{e^{-x} x^{N_r - N_t}}{(N_r - N_t)!}, \quad (12)$$

$$f_{X_{\text{MMSE}}}(x) = \frac{e^{-x}}{\left(1 + \frac{\rho}{N_t} x\right)^{N_t}} \sum_{k=0}^{N_r-1} \beta_k x^{k-1} \left(x \left(1 + \frac{\rho}{N_t} (N_t + x - 1) \right) - k - \frac{\rho k x}{N_t} \right) \quad (13)$$

and

$$f_{X_{\text{MRC}}}(x) = \frac{e^{-x}}{\left(1 + \frac{\rho}{N_t} x\right)^{N_t}} \sum_{k=0}^{N_r-1} \sum_{p=0}^k \frac{\alpha_{p,k} x^{k-1}}{\left(1 + \frac{\rho}{N_t} x\right)^p} \left(x \left(1 + \frac{\rho}{N_t} (N_t - 1 + p + x) \right) - k - \frac{k x \rho}{N_t} \right). \quad (14)$$

In the next two sections, we analyze the maximum sum-rate of the three linear receivers using two different scheduling algorithms which differ depending on whether or not there is SINR feedback from the different users to the transmitter. We present exact and approximate results, and compare the performance of the three linear receivers. Note that we assume all users employ the same receiver structure (ie. ZF, MMSE, or MRC).

III. SCHEDULING WITHOUT FEEDBACK

For multiuser MIMO systems with no feedback capabilities, we consider a simple scheduling algorithm where each transmit antenna is assigned to users in a round robin manner. This includes any scenario where each user is served by each transmit antenna for equal time periods and the data streams received by the users are decoded independently. We consider the practical scenario where the number of users is greater than the number of transmit antennas. The maximum sum-rate under this scheduling scheme is given by

$$R^{\text{rr}}(\rho) = N_t \mathbb{E}_X \left[\log_2 \left(1 + \frac{\rho}{N_t} X \right) \right] \quad (15)$$

where the distribution of X is given in (7), (8) and (10) for the ZF, MMSE and MRC receivers respectively. Note that this is statistically equivalent to the maximum sum-rate of a single user MIMO spatial multiplexing system with linear receivers. Although these systems have been studied extensively, there still remains important open work in this area. Specifically, in this section we present new exact and high SNR closed-form expressions for the maximum sum-rate in (15) with MRC and MMSE receivers. We also present a new analysis of the maximum

sum-rate for each of the three linear receivers in the low SNR regime.

A. Exact Maximum Sum-Rate Results

The exact maximum sum-rate of MIMO systems with ZF receivers has been derived previously (see eg. [8, 9]), and is given by

$$R_{\text{ZF}}^{\text{rr}}(\rho) = \log_e 2 \left(\frac{N_t}{\rho} \right)^{N_r - N_t + 1} N_t e^{\frac{N_t}{\rho}} \sum_{n=1}^{N_r - N_t + 1} \left(\frac{\rho}{N_t} \right)^n \Gamma \left(n - N_r + N_t - 1, \frac{N_t}{\rho} \right) \quad (16)$$

where $\Gamma(\cdot, \cdot)$ is the incomplete gamma function [15]. For MMSE and MRC receivers however, the corresponding expressions are not available. To derive these new results, we find it useful to re-express the maximum sum-rate expression in (15), as given by the following lemma.

Lemma 1: The round robin maximum sum-rate can be written as

$$R^{\text{rr}}(\rho) = \rho \log_e 2 \int_0^\infty \frac{1 - F_X(x)}{1 + \frac{\rho}{N_t} x} dx. \quad (17)$$

Proof: The proof follows by applying integration by parts to (15). ■

In Appendix B, we employ Lemma 1 to derive the exact maximum sum-rate of MRC receivers as follows

$$\begin{aligned} R_{\text{MRC}}^{\text{rr}}(\rho) = \log_e 2 \left(\frac{N_t}{\rho} \right)^{N_t - 1} N_t e^{\frac{N_t}{\rho}} \sum_{k=0}^{N_r - 1} \sum_{p=0}^k \alpha_{p,k} \left(\frac{N_t}{\rho} \right)^k \\ \times \sum_{q=0}^k \binom{k}{q} (-1)^{k-q} \left(\frac{N_t}{\rho} \right)^{p-q} \Gamma \left(1 - N_t - p + q, \frac{N_t}{\rho} \right). \end{aligned} \quad (18)$$

Using a similar approach (we omit the specific details), it can be shown that the exact maximum sum-rate of MMSE receivers is given by

$$\begin{aligned} R_{\text{MMSE}}^{\text{rr}}(\rho) = \log_e 2 \left(\frac{N_t}{\rho} \right)^{N_t - 1} N_t e^{\frac{N_t}{\rho}} \sum_{k=0}^{N_r - 1} \beta_k \left(\frac{N_t}{\rho} \right)^k \\ \times \sum_{q=0}^k \binom{k}{q} (-1)^{k-q} \left(\frac{\rho}{N_t} \right)^q \Gamma \left(1 - N_t + q, \frac{N_t}{\rho} \right). \end{aligned} \quad (19)$$

Fig. 1 compares the analytical maximum sum-rate for MRC, MMSE and ZF based on (18), (19) and [8, Eq. 6] respectively. Monte Carlo simulated curves are also presented for further verification. As expected, we see that the maximum sum-rate of MMSE is greater than for MRC and ZF for all SNR values. We also see an SNR crossover point, such that the maximum sum-rate of MRC is greater than ZF below the crossover point and less than ZF above the crossover

point. This crossover point occurs because the SNR of MRC and ZF approaches that of MMSE, the optimal linear receiver, at low and high SNR respectively.

We numerically calculate this ZF-MRC SNR crossover point in Fig. 2, for different antenna configurations using the maximum sum-rate expressions for MRC in (18) and ZF in [8, Eq. 6]. We see that for a fixed N_r , increasing N_t increases the crossover point, however for a fixed N_t , increasing N_r decreases the crossover point. We also see that the performance of MRC is better than ZF for a number of practical scenarios. For example, when $N_r = N_t = 4$, the MRC maximum sum-rate is greater than the ZF maximum sum-rate for SNR values as high as 8 dB.

We now compare the maximum sum-rate of MRC and MMSE using the analytical expressions in (18) and (19) respectively. Figs. 3, 4 and 5 show the percentage of maximum sum-rate achieved by using an MRC receiver with respect to the MMSE receiver (i.e. $\frac{R_{\text{MRC}}^{\text{rr}}(\rho)}{R_{\text{MMSE}}^{\text{rr}}(\rho)} \times 100$) for different antenna configurations. We see in Fig. 3 that when $N_r < N_t$, the maximum sum-rate of MRC is comparable to MMSE, and approaches the MMSE maximum sum-rate for increasing N_t . For example, for $N_r = 4$ and $N_t = 7$, the MRC maximum sum-rate achieves over 80% of the MMSE maximum sum-rate for SNR ranges as high as 5 dB. On the other hand, when $N_r \geq N_t$, we notice from Fig. 4 and Fig. 5 that increasing the number of transmit antennas has the detrimental effect of reducing the percentage of maximum sum-rate achievable. This can be explained by the fact that for the MMSE receiver, when $N_r \geq N_t$, there are enough receive antennas to cancel the interference from the transmit antennas, hence adding more transmit antennas does not decrease the SNR as much as it does for the MRC receiver.

B. High SNR Analysis

At high SNR, for antenna configurations with $N_r \geq N_t$, expressions for the maximum sum-rate of MMSE receivers have been derived in [10, Eq. 8.54]. For $N_r < N_t$ however, corresponding results are not available. In this case, the maximum sum-rate of MMSE receivers approach a constant at high SNR. In Appendix C, we derive this constant as follows¹

$$R_{\text{MMSE}}^{\text{rr}}(\rho) = \sum_{k=0}^{N_r-1} \frac{N_t}{N_t - k - 1} + o\left(\frac{1}{\rho}\right). \quad (20)$$

¹ $f(x)=o(g(x))$ means that $\lim_{x \rightarrow \infty} \frac{f(x)}{g(x)} = 0$.

Considering MRC receivers, for $N_t > 1$ the maximum sum-rate also approaches a constant at high SNR. Following a similar approach to that used for the MMSE receiver, we evaluate this constant as follows

$$R_{\text{MRC}}^{\text{rr}}(\rho) = \sum_{k=0}^{N_r-1} \frac{N_t}{N_t + k - 1} + o\left(\frac{\log \rho}{\rho}\right). \quad (21)$$

For $N_t \leq N_r$, the maximum sum-rate of ZF and MMSE scales logarithmically with the SNR [10, Eq. 8.54] instead of approaching a constant, and hence always performs better than MRC as expected. From (20) and (21), this can also be shown to be the case when $N_t > N_r$, where the maximum sum-rate of MMSE outperforms MRC. However, (20) and (21) reveal the interesting fact that for high SNR, if N_r is kept fixed and $N_t \rightarrow \infty$, the maximum sum-rate of MRC approaches that of MMSE. This can be intuitively explained by noting that for MMSE, when $N_t > N_r$, there is not enough degrees of freedom for the receiver to cancel the interference imposed by the transmit antennas. Therefore, as N_t grows large, both MMSE and MRC suffer significant interference penalty. As such, for sufficiently large N_t , the interference cancelation capabilities of MMSE become insignificant, and the performance of the two receivers coincide.

The accuracy of (20) and (21) is confirmed in the "Analytical (High SNR)" curves of Fig. 6, where we plot these expressions (without the $o(\cdot)$ terms) as well as Monte Carlo simulated curves. For all cases considered, we see that the Monte Carlo simulated curves converge to the analytical asymptotic results in the high SNR regime. In addition, we also plot the exact "Analytical" curves from (18) and (19), and see an exact match with the Monte Carlo simulated curves.

C. Low SNR Analysis

We now investigate the maximum sum-rate of the three linear receivers in the low SNR regime. The simplest approach is to derive a first order Taylor expansion of $R(\rho)$ as $\rho \rightarrow 0$. It is shown in [16] however, that such an approach does not adequately reveal the impact of the channel, and may in fact lead to misguided conclusions. Moreover, as discussed in detail in [16], in the low SNR (or wideband) regime it is more appropriate to investigate the maximum sum-rate in terms of the normalized transmit energy per information bit, $\frac{E_b}{N_0}$, rather than SNR. In this case

the maximum sum-rate representation is given for low $\frac{E_b}{N_0}$ levels by the following expression

$$R\left(\frac{E_b}{N_0}\right) \triangleq S_0 \frac{\left.\frac{E_b}{N_0}\right|_{\text{dB}} - \left.\frac{E_b}{N_{0\min}}\right|_{\text{dB}}}{3 \text{ dB}} + o\left(\left.\frac{E_b}{N_0}\right|_{\text{dB}} - \left.\frac{E_b}{N_{0\min}}\right|_{\text{dB}}\right) \quad (22)$$

where $\frac{E_b}{N_{0\min}}$ is the minimum normalized energy per information bit required to convey any positive rate reliably, and S_0 is the wideband slope in bits/sec/Hz/(3 dB) at the point $\frac{E_b}{N_{0\min}}$. Note that S_0 and $\frac{E_b}{N_{0\min}}$ can also be used to determine the bandwidth of a system designed to achieve a certain rate subject to power limitations [16].

Now as $\rho \rightarrow 0$, it can be shown from (3) and (5) that the SINR, and hence the maximum sum-rate, of the MMSE and MRC receivers coincide. In Appendix D we derive closed-form solutions for $\frac{E_b}{N_{0\min}}$ and S_0 for both MRC and MMSE as

$$\frac{E_b^{\text{MRC/MMSE}}}{N_{0\min}} = \frac{\ln 2}{N_r} \quad (23)$$

and

$$S_0^{\text{MRC/MMSE}} = \frac{2N_t N_r}{2N_t + N_r - 1} \quad (24)$$

respectively. For ZF receivers, we derive $\frac{E_b}{N_{0\min}}$ and S_0 as

$$\frac{\ln 2}{N_r} \leq \frac{E_b^{\text{ZF}}}{N_{0\min}} = \frac{\ln 2}{N_r - N_t + 1} \leq \ln 2 \quad (25)$$

and

$$1 \leq S_0^{\text{ZF}} = \frac{2N_t(N_r - N_t + 1)}{N_r - N_t + 2} \leq \frac{2N_t N_r}{N_r + 1} \quad (26)$$

respectively. The proof is omitted due to space limitations, but involves solving (51) using the p.d.f. in (12), along with some algebraic manipulation.

We see from (23) and (25) that $\frac{E_b^{\text{MRC/MMSE}}}{N_{0\min}} \leq \frac{E_b^{\text{ZF}}}{N_{0\min}}$, and from (24) and (26) that $S_0^{\text{MRC/MMSE}} \geq S_0^{\text{ZF}}$; in both cases, with equality if $N_t = 1$. Therefore, as expected, whenever $N_t > 1$, the low SNR maximum sum-rate of the MRC and MMSE receivers always exceeds the maximum sum-rate of ZF. The new results given by (23)–(26) precisely quantify this maximum sum-rate difference. In addition, it is interesting to note that $\frac{E_b^{\text{MRC/MMSE}}}{N_{0\min}}$ depends only on the number of receive antennas, also observed in [17] for optimal receivers, whereas $\frac{E_b^{\text{ZF}}}{N_{0\min}}$ depends on both the number of transmit and receive antennas. In fact, we see that increasing the number of transmit antennas for a fixed number of receive antennas has the negative impact of increasing $\frac{E_b^{\text{ZF}}}{N_{0\min}}$.

IV. SCHEDULING WITH SINR FEEDBACK

For multiuser MIMO systems with feedback capabilities, we consider a low-rate feedback approach where each user sends to the transmitter a set of N_t instantaneous SINR values. These correspond to the instantaneous SINRs at the output of the linear receiver; one for each transmit antenna. Specifically, depending on the particular linear receiver employed, the SINRs are calculated based on the average SNR and the channel matrix, according to either (3), (4) or (5), for MRC, ZF, and MMSE respectively; assuming the signal from one antenna is the desired signal while the signals from the other antennas are interference.

We employ an opportunistic scheduling algorithm which selects, for each transmit antenna, the user with the maximum SINR. Note that each user can be served by more than one transmit antenna, ie. multiple data streams can be sent to a single user. The maximum sum-rate can be written as

$$\begin{aligned}
 R^{\max}(\rho) &= \sum_{i=1}^{N_t} \mathbb{E}_{X_{\max}} \left[\log_2 \left(1 + \frac{\rho}{N_t} X_{\max} \right) \right] \\
 &= N_t \mathbb{E}_{X_{\max}} \left[\log_2 \left(1 + \frac{\rho}{N_t} X_{\max} \right) \right] \\
 &= N_t K \int_0^{\infty} \log_2(1+x) f_X(x) F_X^{K-1}(x) dx
 \end{aligned} \tag{27}$$

where $X_{\max} = \max_{1 \leq i \leq K} X_i$ and f_X and F_X are given for MRC, ZF and MMSE in (7)-(14). In the following, we derive new accurate approximations for (27) for MRC, ZF and MMSE receivers. Note that, for the case of ZF, exact expressions have been derived previously in [8]. Those results, however, incurred high computational complexity which increased significantly with the number of users and, as such, would take time comparable to Monte Carlo simulations to produce meaningful plots. As such, we are motivated to consider deriving simpler, more computationally-efficient, accurate approximations for the ZF receiver as well.

A. Maximum Sum-Rate Approximations

To obtain closed form expressions for the maximum sum-rate of the linear receivers, we can directly evaluate the integral in (27) by first substituting the c.d.f. expressions in (7), (8) and (10), along with the corresponding p.d.f. expressions in (12)-(14) into (27). We can then apply the multinomial theorem and evaluate the resulting integral using standard identities from [18].

However, although this approach produces an exact closed-form solution, the resulting expression has a complexity which increases significantly with the number of users K , and would take time comparable to Monte Carlo simulations to produce meaningful plots for even small K values (eg. $K = 10$). As such, we are well motivated to consider accurate approximations for the maximum sum-rate, which have much lower computational complexity requirements. Our approach is to approximate (27) by the following

$$R^{\max}(\rho) \approx N_t \log_2 \left(1 + \frac{\rho}{N_t} g(K) \right) \quad (28)$$

where²

$$g(K) = F_X^{-1} \left(\frac{1}{1 + e^{-\sum_{i=1}^{K-1} \frac{1}{i}}} \right) \quad (29)$$

with the distribution of X given in (7), (8) and (10) for the ZF, MMSE and MRC receivers respectively. This expression is obtained by first noting that for a random variable Y following a symmetric distribution, with c.d.f. $F_Y(\cdot)$ and largest order statistic Y_K , the following inequality holds [19]

$$\mathbb{E}[Y_K] \leq F_Y^{-1} \left(\frac{1}{1 + e^{-\sum_{i=1}^{K-1} \frac{1}{i}}} \right). \quad (30)$$

To obtain (28), we substitute $Y = N_t \log_2 \left(1 + \frac{\rho}{N_t} X \right)$ into (30), and apply simple algebraic manipulation.

We note that this general upper bounding approach has been shown to be tight for a Gaussian distribution [20]. We would therefore expect it to be tight in (28) also, at least at low SNR values, upon noting that for low SNR we have $\log_2 \left(1 + \frac{\rho}{N_t} X \right) \approx \frac{\rho}{N_t} X$, which has been shown to converge to a Gaussian distribution as $N_t, N_r \rightarrow \infty$ for MRC, ZF and MMSE [21, 22]. This expected tightness is confirmed in our numerical results.

We will focus on evaluating (28), and show that it yields an accurate approximation for (27). To calculate (28), we require the inverse function of $F_X(\cdot)$ in $g(K)$. Unfortunately, for ZF, MMSE and MRC, the c.d.f.s in (7), (8) and (10) respectively, are in a form for which the inverse c.d.f. is difficult to obtain. We thus employ a simple numerical algorithm, similar that considered in

²Note that throughout this paper, we will use F^{-1} to denote the inverse function of F , and F^N to indicate the N th power. There is no contradiction in this notation since we only consider positive powers in this paper.

[23], to evaluate $g(K) = F_X^{-1} \left(\frac{1}{1+e^{-\sum_{i=1}^{K-1} \frac{1}{i}}} \right)$. In particular, we start with $g_0(K) = 1$, and iterate the following expression

$$g_{j+1}(K) = \ln(N(K)) + \ln(1 - F_X(g_j(K))) + g_j(K) \quad (31)$$

until convergence, where $N(K) = 1 + e^{\sum_{i=1}^{K-1} \frac{1}{i}}$, and $F_X(\cdot)$ is given in (7), (8) and (10) for ZF, MMSE and MRC receivers respectively. Note that the algorithm will eventually converge, because additional iterations of (31) results in additional nested logarithms, which contribute less and less to the outermost logarithm, ie. the logarithm at the first iteration at $j = 0$.

Simulations indicate that (31) has a fast rate of convergence. The exact rate, however, depends on the number of antennas and linear receiver used in the system. Table I shows the absolute error percentage versus the number of iterations, for the MMSE receiver and for different antenna configurations. The absolute error percentages were calculated by using the algorithm in (31) and numerical results from the exact c.d.f. in (8). We see that the convergence rate is fast in all cases.

We denote $g_{\text{conv}}(K)$ to be the converged value from (31). Substituting this into (28) in place of $g(K)$ gives an approximation to maximum sum-rate as follows

$$R^{\max}(\rho) \approx N_t \log_2 \left(1 + \frac{\rho}{N_t} g_{\text{conv}}(K) \right). \quad (32)$$

Fig. 7 compares the analytical approximations for MRC, ZF and MMSE with Monte Carlo simulated curves. The analytical approximation curves were obtained using (7), (8), (10), (31) and (32). We see that these curves accurately approximate the Monte Carlo simulated curves in all cases.

B. Large User Analysis

We now examine the maximum sum-rate for MRC, ZF and MMSE, in the *large-K* regime .

Theorem 1: For sufficiently large K , the maximum sum-rate for the MRC, ZF, and MMSE receivers is given by

$$\begin{aligned} R^{\max}(\rho) = & N_t \log_2 \ln K + N_t \log_2 \rho - N_t \log_2 N_t \\ & + N_t \log_2 \left(\frac{\ln(\alpha)\rho}{N_t \ln K} + 1 + \frac{1}{\ln K} \left(1 + \frac{\rho(N_r - N_t)\mathcal{O}(\ln \ln K)}{N_t} \right) \right) \end{aligned} \quad (33)$$

where α is given for MRC, ZF and MMSE as follows

$$\alpha = \begin{cases} \frac{\left(\frac{N_t}{\rho}\right)^{N_t-1}}{(N_r-1)!} & \text{MRC} \\ \frac{1}{(N_r-N_t)!} & \text{ZF} \\ \sum_{p=\max(0, N_r-N_t)}^{N_r-1} \frac{\binom{N_t-1}{N_r-1-p} \left(\frac{\rho}{N_t}\right)^{N_r-N_t-p}}{p!} & \text{MMSE} . \end{cases} \quad (34)$$

Proof: See Appendix E. ■

Corollary 1: For even larger K , the maximum sum-rate (33) becomes

$$R^{\max}(\rho) = N_t (\log_2 \ln K + \log_2 \rho - \log_2 N_t) + \mathcal{O}\left(\frac{\ln \ln K}{\ln K}\right). \quad (35)$$

Proof: The proof follows by applying basic algebraic manipulation to (33). ■

Note that for the case of ZF receivers, an upper bound to (35) was derived in [11], and for the case of MRC and MMSE receivers with $N_t = 4$ and $N_r = 2$, the exact maximum sum-rate scaling law was reported in [12]. As such, our expressions generalize these prior results by giving exact scaling laws for all three receivers, which apply for arbitrary numbers of antennas. Our results also yield important insights into the fundamental differences in terms of maximum sum-rate scaling for each of the three linear receivers.

From Corollary 1, we see that the maximum sum-rate for all three receivers follow the same asymptotic scaling law with respect to the number of users. The key difference, however, is demonstrated by Theorem 1, where the *rate of maximum sum-rate increase* with K is seen to be a decreasing function of α . That is, although the linear receivers follow the same asymptotic scaling law, the speed at which that law is approached varies with α , which depends on the particular receiver structure.

In general terms, we see from (33) that for large but finite numbers of users K , the maximum sum-rate is a monotonically increasing function of α . From (34), we clearly see that $\alpha_{\text{MMSE}} > \alpha_{\text{MRC}}$ and $\alpha_{\text{MMSE}} > \alpha_{\text{ZF}}$. We also have $\alpha_{\text{MRC}} > \alpha_{\text{ZF}}$ if

$$\rho \leq N_t \left(\frac{(N_r - N_t)!}{(N_r - 1)!} \right)^{\frac{1}{N_t-1}} \quad (36)$$

and $\alpha_{\text{ZF}} \geq \alpha_{\text{MRC}}$ otherwise. Therefore, for large K , (36) represents the SNR crossover point between the maximum sum-rate of ZF and MRC receivers, discussed in Section III-A. We note that the right-hand-side of (36) is a decreasing function of the number of receive antennas. This is consistent with the behavior of the corresponding ZF-MRC SNR crossing point for the

round-robin scheduler, observed in Section III-A.

Note that although this convergence behavior of the three linear receivers is not readily apparent from the results in Fig. 7, for the finite numbers of users considered, it can be clearly seen in Fig. 8, where we plot the difference in maximum sum-rate between the MMSE and MRC receivers (i.e. $R_{\text{MMSE}}^{\max}(\rho) - R_{\text{MRC}}^{\max}(\rho)$) as a function of the number of users using (32). We clearly see that the difference in maximum sum-rate is a decreasing function of the number of users.

The fact that all three linear receivers converge in the limit as $K \rightarrow \infty$ can be intuitively explained as follows. The performance in each case is limited by the interference from the other transmit antennas. As $K \rightarrow \infty$, the probability of the opportunistic scheduling algorithm choosing a user such that the interference is negligible approaches one. In this interference-free scenario, all linear receivers thus have the same performance, and the SINRs all converge to the same value, i.e. $\gamma_{\text{MRC}} \rightarrow \gamma_{\text{ZF}} \rightarrow \gamma_{\text{MMSE}}$ as $K \rightarrow \infty$.

We see in Fig. 7 that the opportunistic scheduler can provide a significant increase in maximum sum-rate compared to a round robin scheduler (i.e. corresponding to the point $K = 1$); at the expense of requiring more SINR feedback. It is also worth noting that when the users are stationary, fairness may become an issue for the SINR-based scheduler, since the transmitter is likely to send to a subset of users for the majority of the time. When the users are sufficiently mobile, however, such that the channel realizations change for each transmission period, then on average each user will be served for approximately equal amounts of time under the opportunistic SINR-based scheduling approach.

V. CONCLUSION

We have analyzed the maximum sum-rate of MRC, ZF and MMSE receivers in MIMO multiuser systems. We considered two scheduling algorithms, which differ depending on whether or not there is SINR feedback at the transmitter. When there is no feedback, we considered a simple round-robin scheduling algorithm, deriving new exact closed-form maximum sum-rate expressions for the MRC and MMSE receivers for arbitrary SNRs, and simplified results in the high SNR regime. We also investigated the maximum sum-rate of all three linear receivers in the low SNR regime. When there is feedback, we considered a simple opportunistic scheduling algorithm based on exploiting SINR feedback from the receivers to the transmitter. We derived

new accurate maximum sum-rate approximations and exact maximum sum-rate scaling laws for the MRC, ZF and MMSE receivers. Our results demonstrated that all three linear receivers obeyed the same asymptotic scaling law, however the rate of convergence differed based on a simple intuitive parameter α , which we quantified. Our results were confirmed through comparison with Monte Carlo simulations.

APPENDIX

A. Proof of the SINR C.D.F. with MRC

The normalized SINR X_{MRC} can be written as

$$X_{\text{MRC}} = \frac{|\mathbf{h}_{i,k}^\dagger \mathbf{h}_{i,k}|}{\frac{\rho}{N_t} \sum_{j=1, j \neq k}^{N_t} \frac{|\mathbf{h}_{i,k}^\dagger \mathbf{h}_{i,j}|^2}{|\mathbf{h}_{i,k}^\dagger \mathbf{h}_{i,k}|} + 1} = \frac{Z}{Y + 1} \quad (37)$$

where Z is a chi-squared distribution with $2N_r$ degrees of freedom with c.d.f.

$$F_Z(z) = 1 - e^{-z} \sum_{k=0}^{N_r-1} \frac{z^k}{k!} \quad (38)$$

and Y is a chi-squared distribution with $2(N_t - 1)$ degrees of freedom with p.d.f. [24]

$$f_Y(y) = \frac{y^{N_t-2} e^{-\frac{yN_t}{\rho}}}{\Gamma(N_t - 1) \left(\frac{\rho}{N_t}\right)^{N_t-1}}. \quad (39)$$

The c.d.f. of X_{MRC} can be written as

$$\begin{aligned} F_{X_{\text{MRC}}}(x) &= \Pr(X_{\text{MRC}} < x) \\ &= \int_0^\infty \Pr(Z < x(y+1)) f_Y(y) dy \\ &= 1 - \frac{e^{-x}}{\Gamma(N_t - 1) \left(\frac{\rho}{N_t}\right)^{N_t-1}} \sum_{k=0}^{N_r-1} \frac{x^k}{k!} \sum_{p=0}^k \binom{k}{p} \int_0^\infty e^{-y(x+\frac{N_t}{\rho})} y^{N_t-2+p} dy. \end{aligned} \quad (40)$$

Finally, we obtain the desired result by first solving the integral in (40) using identities in [18] followed by some algebraic manipulation.

B. Proof of the MRC Maximum Sum-Rate with Round Robin Scheduler

Substituting (10) into (17), we can write the maximum sum-rate of MRC as

$$R_{\text{MRC}}^{\text{rr}}(\rho) = \sum_{k=0}^{N_r-1} \sum_{p=0}^k \alpha_{p,k} \int_0^\infty \frac{e^{-x} x^k}{\left(1 + \frac{\rho}{N_t} x\right)^{N_t+p}} dx$$

$$= e^{\frac{N_t}{\rho}} \sum_{k=0}^{N_r-1} \sum_{p=0}^k \frac{\alpha_{p,k} N_t^{k+1}}{\rho^{k+1}} \sum_{q=0}^k \binom{k}{q} (-1)^{k-q} \int_1^\infty y^{q-p-N_t} e^{-\frac{y N_t}{\rho}} dy \quad (41)$$

where the first line follows using integration by parts, and the integral in the last line is solved using integral identities in [18].

C. Proof of MMSE Maximum Sum-Rate at High SNR for $N_t > N_r$

We first write the maximum sum-rate in (19) as

$$R_{\text{MMSE}}^{\text{rr}}(\rho) = N_t \sum_{k=0}^{N_r-1} \sum_{p=\max(0, k-N_t+1)}^k \frac{\binom{N_t-1}{k-p}}{p!} \sum_{q=0}^k \binom{k}{q} (-1)^{k-q} \theta(\rho) \quad (42)$$

where

$$\theta(\rho) = e^{\frac{N_t}{\rho}} \left(\frac{N_t}{\rho} \right)^\kappa \Gamma \left(1 - N_t + q, \frac{N_t}{\rho} \right) \quad (43)$$

and $\kappa = N_t - q - 1 + p$. To obtain high SNR maximum sum-rate expressions for (42), we require the limiting behavior of $\Gamma \left(1 - N_t + q, \frac{N_t}{\rho} \right)$ as $\rho \rightarrow \infty$. This is given by [15]

$$\begin{aligned} \lim_{\rho \rightarrow \infty} \Gamma \left(1 - N_t + q, \frac{N_t}{\rho} \right) &= \frac{(-1)^{N_t-1-q}}{(N_t-1-q)!} \left(\phi(N_t - q) - \log \left(\frac{N_t}{\rho} \right) \right) \\ &\quad + \frac{\left(\frac{N_t}{\rho} \right)^{1-N_t+q}}{N_t-1-q} + o \left(\frac{1}{\rho} \right) \end{aligned} \quad (44)$$

where $\phi(\cdot)$ is the digamma function. Substituting (44) into (43), it is convenient to write $\theta(\rho)$ as

$$\theta(\rho) = \theta_1(\rho) + \theta_2(\rho) + o \left(\frac{1}{\rho^{\kappa+1}} \right) \quad (45)$$

where

$$\theta_1(\rho) = \left(\frac{N_t}{\rho} \right)^\kappa \frac{(-1)^{N_t-1-q}}{(N_t-1-q)!} \left(\phi(N_t - q) - \log \left(\frac{N_t}{\rho} \right) \right) \quad (46)$$

and

$$\theta_2(\rho) = \frac{\left(\frac{N_t}{\rho} \right)^p}{N_t-1-q} . \quad (47)$$

We proceed by first analyzing the high SNR performance of θ_1 and θ_2 in (46) and (47). For θ_1 , as $q < N_t - 1$ we are only required to find the minimum exponent of $\frac{N_t}{\rho}$ in (46), i.e. minimum κ . This occurs when $q = N_r - 1$, so that $\kappa = N_t - N_r + p$. Clearly, for any value of $p \geq 0$,

$$\theta_1(\rho) = o \left(\frac{\log \rho}{\rho} \right) . \quad (48)$$

We now consider $\theta_2(\rho)$. For large SNR, we only need to consider the smallest exponent of p in (47), i.e. $p = 0$. This gives

$$\theta_2(\rho) = \frac{1}{N_t - q - 1} + o\left(\frac{1}{\rho}\right). \quad (49)$$

Substituting (48) and (49) into (43), and then using the resulting expression in (42), we obtain the maximum sum-rate as

$$R_{\text{MMSE}}^{\text{rr}}(\rho) = N_t \sum_{k=0}^{N_r-1} \binom{N_t-1}{k} \sum_{q=0}^k \binom{k}{q} \frac{(-1)^{k-q}}{N_t - q - 1} + o\left(\frac{\log \rho}{\rho}\right) = \sum_{k=1}^{N_r} \frac{1}{1 - \frac{k}{N_t}} + o\left(\frac{\log \rho}{\rho}\right) \quad (50)$$

where the last equality follows after some simple algebraic manipulation.

D. Proof of Low SNR Results

From [16], $\frac{E_b}{N_0 \min}$ and S_0 are given respectively by

$$\frac{E_b}{N_0 \min} = \frac{\ln 2}{\dot{R}^{\text{rr}}(0)} \quad \text{and} \quad S_0 = -\frac{2 \ln 2 [\dot{R}^{\text{rr}}(0)]^2}{\ddot{R}^{\text{rr}}(0)} \quad (51)$$

where $\dot{R}(\cdot)$ and $\ddot{R}(\cdot)$ denote the first and second derivative of $R(\cdot)$ respectively w.r.t. ρ .

We start with the derivation of $\frac{E_b}{N_0 \min}$ and S_0 for the MRC receiver. Substituting (3) into (15) and taking the derivative w.r.t. ρ , we find that

$$\dot{R}_{\text{MRC}}^{\text{rr}}(0) = \log_2(e) \mathbb{E} \left[|\mathbf{h}_{i,k}^\dagger \mathbf{h}_{i,k}| \right] = N_r \log_2(e). \quad (52)$$

Similarly, taking the second derivative of $R_{\text{MRC}}^{\text{rr}}$ w.r.t. ρ , we obtain

$$\begin{aligned} \ddot{R}_{\text{MRC}}^{\text{rr}}(0) &= -\frac{\log_2(e)}{N_t} \mathbb{E} \left[|\mathbf{h}_{i,k}^\dagger \mathbf{h}_{i,k}| \left(|\mathbf{h}_{i,k}^\dagger \mathbf{h}_{i,k}| + 2 \sum_{j=1, j \neq k}^{N_t} \frac{|\mathbf{h}_{i,k}^\dagger \mathbf{h}_{i,j}|^2}{|\mathbf{h}_{i,k}^\dagger \mathbf{h}_{i,k}|} \right) \right] \\ &= -\frac{\log_2(e) N_r (2N_t + N_r - 1)}{N_t} \end{aligned} \quad (53)$$

where we have used (38) and (39). Substituting (52) and (53) into (51), we obtain the desired result.

Now consider the MMSE receiver. In this case, it is convenient to write

$$R_{\text{MMSE}}^{\text{rr}}(\rho) = N_t \log_2 \left(1 - \sum_{i=0}^{\infty} \left(-\frac{\rho}{N_t} \right)^{i+1} \mathbf{h}_{i,k}^\dagger (\mathbf{K} \mathbf{K}^\dagger)^i \mathbf{h}_{i,k} \right) \quad (54)$$

which is obtained by substituting (5) into (15), and using [25]. In this form, we can calculate

the required first and second order derivatives as follows

$$\dot{R}_{\text{MMSE}}^{\text{rr}}(0) = \log_2(e) \mathbb{E} \left[\mathbf{h}_{i,k}^\dagger \mathbf{h}_{i,k} \right] = N_r \log_2(e) \quad (55)$$

and

$$\ddot{R}_{\text{MMSE}}^{\text{rr}}(0) = -\frac{\log_2(e)}{N_t} \mathbb{E} \left[\left(2\mathbf{h}_{i,k}^\dagger \mathbf{K} \mathbf{K}^\dagger \mathbf{h}_{i,k} + \left(\mathbf{h}_{i,k}^\dagger \mathbf{h}_{i,k} \right)^2 \right) \right]. \quad (56)$$

To solve (58), we write

$$\begin{aligned} \mathbb{E} \left[\mathbf{h}_{i,k}^\dagger \mathbf{K} \mathbf{K}^\dagger \mathbf{h}_{i,k} \right] &= \text{Tr} \left(\mathbb{E} \left[\mathbf{h}_{i,k}^\dagger \mathbf{K} \mathbf{K}^\dagger \mathbf{h}_{i,k} \right] \right) \\ &= \text{Tr} \left(\mathbb{E} \left[\mathbf{K}^\dagger \mathbf{h}_{i,k} \mathbf{h}_{i,k}^\dagger \mathbf{K} \right] \right) \\ &= 2(N_t - 1)N_r \end{aligned} \quad (57)$$

where we have used [26, Theorem 2.3.5]. Substituting (57) into (56) gives

$$\begin{aligned} \ddot{R}_{\text{MMSE}}^{\text{rr}}(0) &= -\frac{\log_2(e)}{N_t} (2(N_t - 1)N_r + N_r(N_r + 1)) \\ &= -\frac{\log_2(e)N_r (2N_t + N_r - 1)}{N_t}. \end{aligned} \quad (58)$$

Finally, substituting (55) and (58) into (51), we obtain the desired result.

E. Proof of Theorem 1

We first give the following lemma:

Lemma 2: For sufficiently large K ,

$$R^{\text{max}}(\rho) = \log_2 \left(1 + \frac{\rho}{N_t} F_X^{-1} \left(\frac{K}{K+1} \right) \right). \quad (59)$$

Proof: The proof follows by applying a general result from order statistics [19] to $C_X^{\text{max}}(\rho)$ in (27), and performing some simple algebraic manipulation. ■

Lemma 2 implies that for large K , we need only consider the c.d.f. in (10), (7) and (8) in the high x regime. By consider the expressions for the largest exponents of x in (10), (7) and (8), followed by some algebraic manipulation, this is given for MRC, ZF and MMSE respectively as

$$F_{X_{\text{MRC}}}(x) = 1 - \frac{e^{-x} x^{N_r - N_t} \left(\frac{N_t}{\rho} \right)^{N_t - 1}}{(N_r - 1)!} + o(x^{N_r - N_t - 1}) \quad (60)$$

$$F_{X_{ZF}}(x) = 1 - \frac{e^{-x}x^{N_r-N_t}}{(N_r - N_t)!} + o(x^{N_r-N_t-1}) \quad (61)$$

and

$$F_{X_{MMSE}}(x) = 1 - e^{-x}\beta_{N_r-1}x^{N_r-N_t}\left(\frac{N_t}{\rho}\right)^{N_t-1} + o(x^{N_r-N_t-1}). \quad (62)$$

Note that these c.d.f. expansions are each of the general form $F_X^*(x) = 1 - \alpha e^{-x}x^{N_r-N_t} + o(x^{N_r-N_t-1})$. In addition, these expansions approach the actual c.d.f. (without the $o(\cdot)$ term) for large x . Now, the factor $F_X^{-1}\left(\frac{K}{K+1}\right)$ in (59) can be solved by substituting $N(K) = K+1$ into the iteration (31). As K is large, only one iteration is needed, since more iterations would produce nested \ln terms which have negligible effect. This gives for large K

$$\begin{aligned} R^{\max}(\rho) &= N_t \log_2 \left(1 + \frac{\rho}{N_t} (\ln(\alpha) + \ln(K) + (N_r - N_t)\mathcal{O}(\ln \ln K)) \right) \\ &= N_t \log_2 \ln K + N_t \log_2 \left(\frac{1}{\ln K} + \frac{\rho}{N_t} \left(\frac{\ln(\alpha)}{\ln K} + 1 + \frac{(N_r - N_t)\mathcal{O}(\ln \ln K)}{\ln K} \right) \right). \end{aligned} \quad (63)$$

The proof follows by algebraic manipulation.

REFERENCES

- [1] L.-U. Choi and R. D. Murch, "A transmit preprocessing technique for multiuser MIMO systems using a decomposition approach," *IEEE Trans. Wireless Commun.*, vol. 3, no. 1, pp. 20–24, Jan. 2004.
- [2] N. Jindal and A. Goldsmith, "Dirty-paper coding versus TDMA for MIMO broadcast channels," *IEEE Trans. Inform. Theory*, vol. 51, no. 5, pp. 1783–1794, May 2005.
- [3] K.-K. Wong, R. D. Murch, and K. B. Letaief, "A joint-channel diagonalization for multiuser MIMO antenna systems," *IEEE Trans. Wireless Commun.*, vol. 2, no. 4, pp. 773–786, Jul. 2003.
- [4] T. Yoo and A. Goldsmith, "On the optimality of multiantenna broadcast scheduling using zero-forcing beamforming," *IEEE Sel. Area. Commun.*, vol. 24, no. 3, pp. 528–541, Mar. 2006.
- [5] C. Wang and R. D. Murch, "Adaptive downlink multi-user MIMO wireless systems for correlated channels with imperfect CSI," *IEEE Trans. Wireless Commun.*, vol. 5, no. 9, pp. 2435–2446, Sep. 2006.
- [6] G. J. Foschini and M. J. Gans, "On limits of wireless communications in a fading environment when using multiple antennas," *Wireless Pers. Commun.*, vol. 6, pp. 311–335, Mar. 1998.
- [7] M. R. McKay and I. B. Collings, "General capacity bounds for spatially correlated Rician MIMO channels," *IEEE Trans. Inform. Theory*, vol. 51, no. 9, pp. 3121–3145, Sep. 2005.
- [8] C.-J. Chen and L.-C. Wang, "Performance analysis of scheduling in multiuser MIMO systems with zero-forcing receivers," *IEEE Sel. Area Commun.*, vol. 25, no. 7, pp. 1435–1445, Sep. 2007.

-
- [9] A. Forenza, M. R. McKay, A. Pandharipande, R. W. Heath Jr., and I. B. Collings, "Adaptive MIMO transmission for exploiting the capacity of spatially correlated channels," *IEEE Trans. on Veh. Technol.*, vol. 56, no. 2, pp. 619–630, Mar. 2007.
- [10] D. Tse and P. Viswanath, *Fundamentals of Wireless Communications*, 1st ed. New York: Cambridge, 2005.
- [11] M. Airy, R. W. Heath Jr., and S. Shakkottai, "Multiuser diversity for the multiple antenna broadcast channel with linear receivers: asymptotic analysis," in *Asilomar Conference on Signals, Systems and Computers*, vol. 1, Pacific Grove, California, Nov. 2004, pp. 886–890.
- [12] M.-O. Pun, V. Koivunen, and H. V. Poor, "SINR analysis of opportunistic MIMO-SDMA downlink systems with linear combining," in *IEEE Int. Conf. on Commun. (ICC)*, Beijing, China, May 2008, pp. 3720–3724.
- [13] H. Gao, P. J. Smith, and M. V. Clark, "Theoretical reliability of MMSE linear diversity combining in Rayleigh-fading additive interference channels," *IEEE Trans. Commun.*, vol. 46, no. 5, pp. 666–672, May 1998.
- [14] J. M. Romero-Jerez and A. Goldsmith, "Receive antenna array strategies in fading and interference: An outage probability comparison," *IEEE Trans. Wireless Commun.*, vol. 7, no. 3, pp. 920–932, Mar. 2008.
- [15] M. Abramowitz and I. A. Stegun, *Handbook of Mathematical Functions with Formulas, Graphs, and Mathematical Tables*, 9th ed. New York: Dover Publications, 1970.
- [16] S. Verdú, "Spectral efficiency in the wideband regime," *IEEE Trans. Inform. Theory*, vol. 48, no. 6, pp. 1319–1343, Jun. 2002.
- [17] A. Lozano, A. M. Tulino, and S. Verdú, "Multiple-antenna capacity in the low-power regime," *IEEE Trans. Inform. Theory*, vol. 49, no. 10, pp. 2527–2544, Oct. 2003.
- [18] I. S. Gradshteyn and I. M. Ryzhik, *Table of Integrals, Series, and Products*, 4th ed. San Diego, CA: Academic, 1965.
- [19] W. V. Zwet, *Convex Transformations of Random Variables*. Mathematical Centre, 1970.
- [20] H. David and H. Nagaraja, *Order Statistics*, 3rd ed. New Jersey: John Wiley and Sons, 2003.
- [21] D. Guo, S. Verdú, and L. K. Rasmussen, "Asymptotic normality of linear multiuser receiver outputs," *IEEE Trans. Inform. Theory*, vol. 48, no. 12, pp. 3080–3095, Dec. 2002.
- [22] J. Zhang, E. K. P. Chong, and D. N. C. Tse, "Output MAI distribution of linear MMSE multiuser receivers in DS-CDMA systems," *IEEE Trans. Inform. Theory*, vol. 47, no. 3, pp. 1128–1144, Mar. 2001.
- [23] R. H. Y. Louie, M. R. McKay, and I. B. Collings, "Impact of correlation on the capacity of multiple access and broadcast channels with MIMO-MRC," *IEEE Trans. Wireless Commun.*, vol. 7, no. 6, pp. 2397–2407, Jun. 2008.
- [24] A. Shah and A. M. Haimovich, "Performance analysis of optimum combining in wireless communications with Rayleigh fading and cochannel interference," *IEEE Trans. Commun.*, vol. 46, no. 4, pp. 473–479, Apr. 1998.
- [25] H. Lütkepohl, *Handbook of Matrices*, 1st ed. England: John Wiley and Sons, 1996.
- [26] A. K. Gupta and D. K. Nagar, *Matrix Variate Distributions*. Boca Raton: Chapman & Hall/CRC, 2000.

TABLE I

ABSOLUTE ERROR (%) BETWEEN EXACT INVERSE C.D.F. AND ANALYTICAL VALUES USING THE MMSE RECEIVER FOR
DIFFERENT ITERATIONS, WITH $K = 4$ AND $\rho = 3$ dB.

Antenna Configuration	1 It.	2 It.	3 It.	4 It.	5 It.	6 It.
$N_t = N_r = 2$	10.3845	0.8346	0.0685	0.0056	0.0005	0.0001
$N_t = N_r = 3$	21.6231	2.7165	0.3519	0.0458	0.0060	0.0008
$N_t = N_r = 4$	32.8893	5.1821	0.8443	0.1383	0.0227	0.0037
$N_t = N_r = 5$	43.9760	8.0287	1.5140	0.2877	0.0547	0.0104

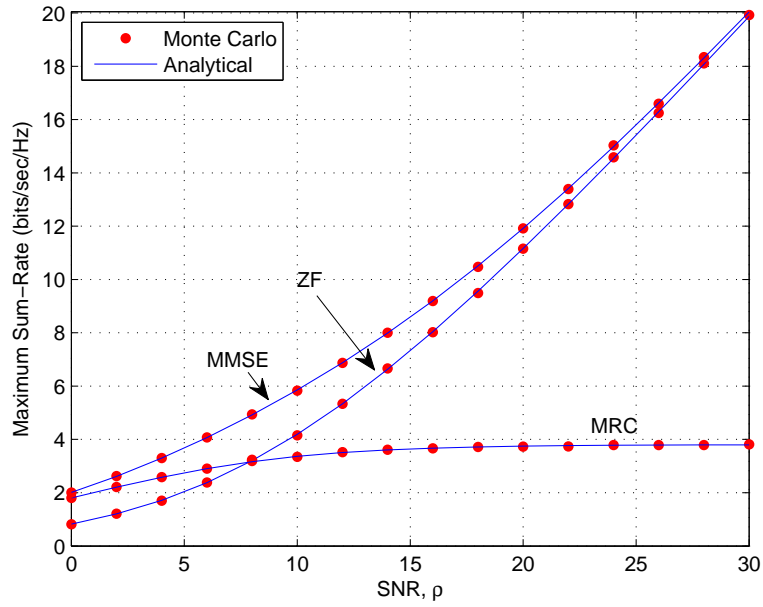


Fig. 1. Maximum sum-rate of MRC, ZF and MMSE using scheduling without feedback. Comparison between analytical and Monte Carlo simulated maximum sum-rate for $N_t = N_r = 4$.

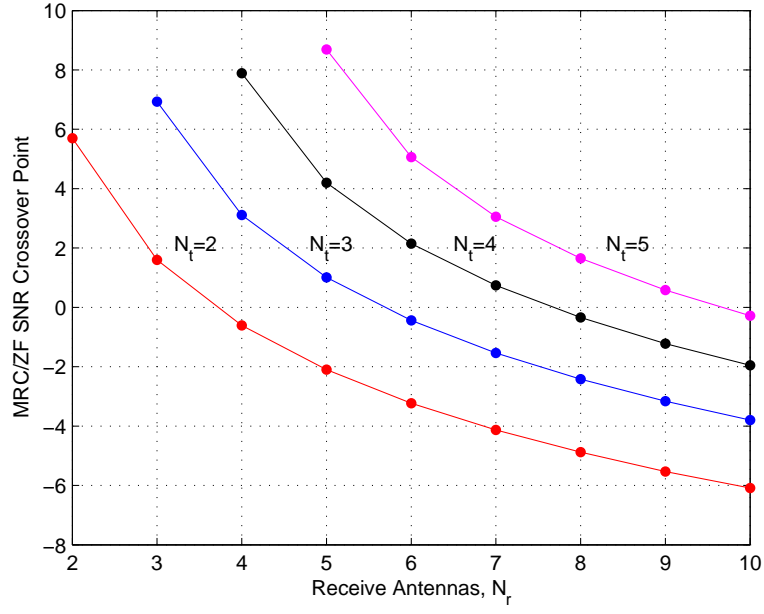


Fig. 2. SNR crossover point where the ZF maximum sum-rate is equal to the MRC maximum sum-rate using scheduling without feedback.

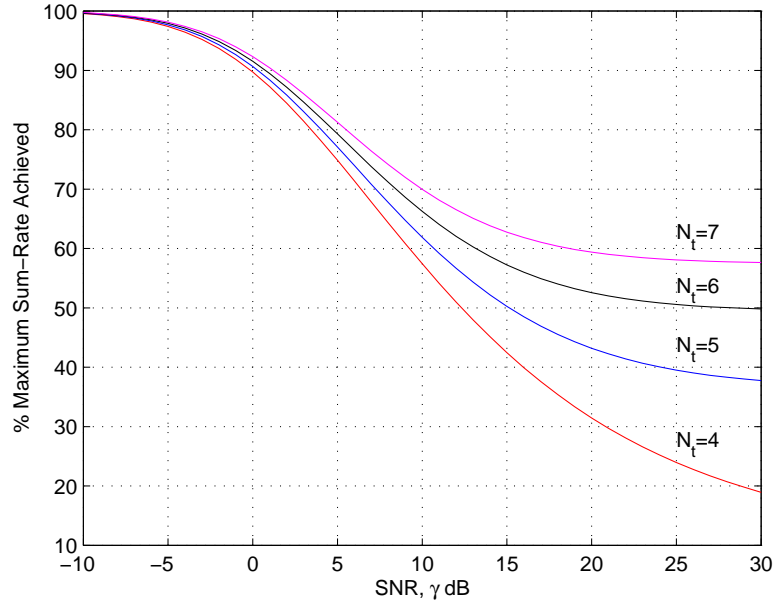


Fig. 3. Percentage of MMSE maximum sum-rate achieved by MRC for $N_r = 4$ using scheduling without feedback.

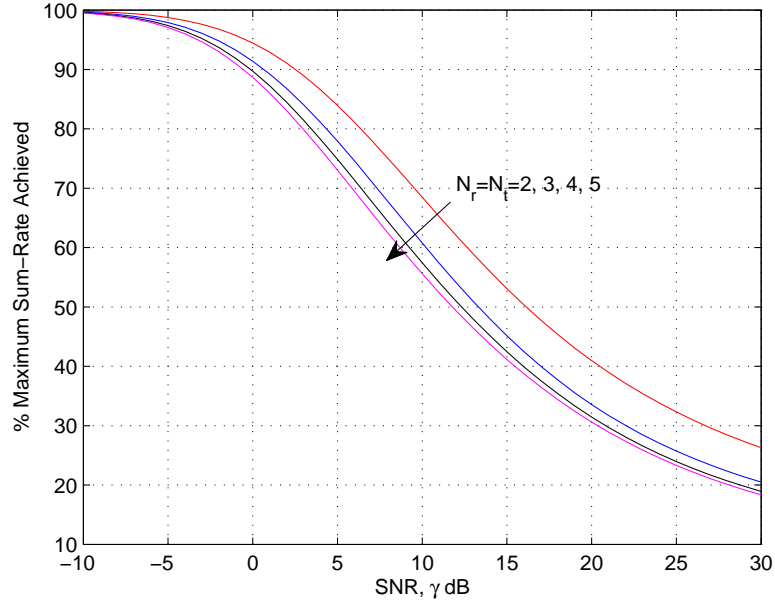


Fig. 4. Percentage of MMSE maximum sum-rate achieved by MRC using scheduling without feedback.

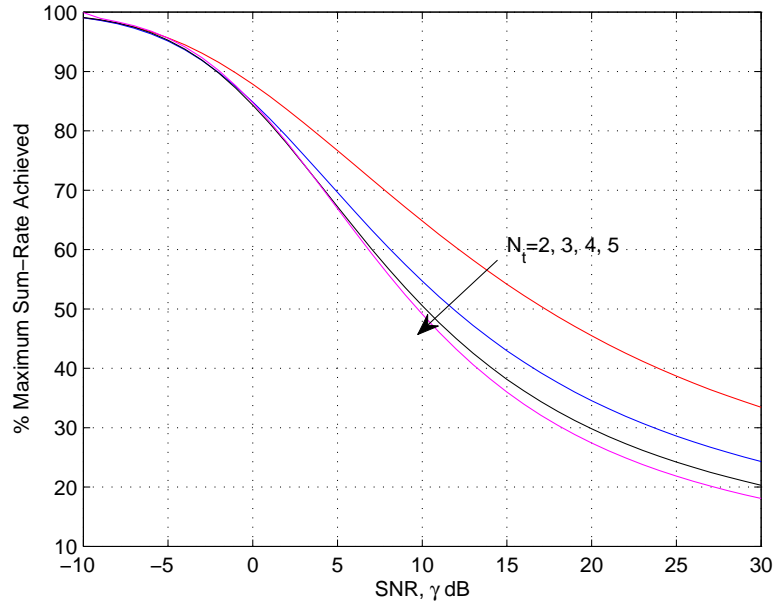


Fig. 5. Percentage of MMSE maximum sum-rate achieved by MRC for $N_r = 8$ using scheduling without feedback.

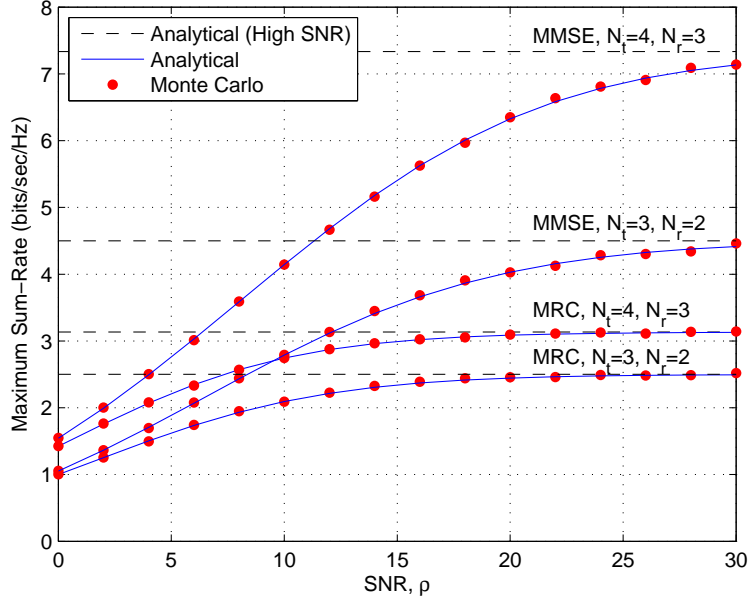


Fig. 6. Maximum sum-rate of MRC and MMSE using scheduling without feedback. Comparison between analytical and Monte Carlo simulated maximum sum-rate for different antenna configurations with $N_t > N_r$, using scheduling without feedback.

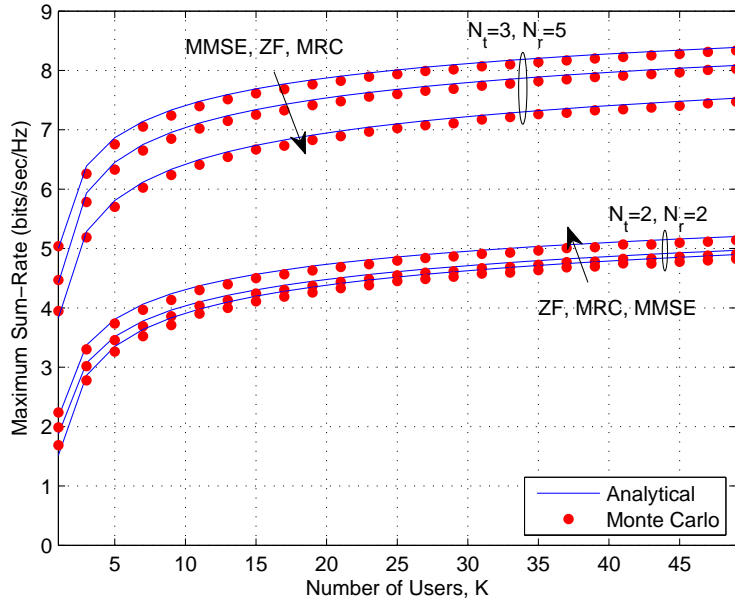


Fig. 7. Maximum sum-rate of MRC, ZF and MMSE using the opportunistic scheduler with SINR feedback. Comparison between analytical and Monte Carlo simulated maximum sum-rate for different antenna configurations with $\rho = 3$ dB.

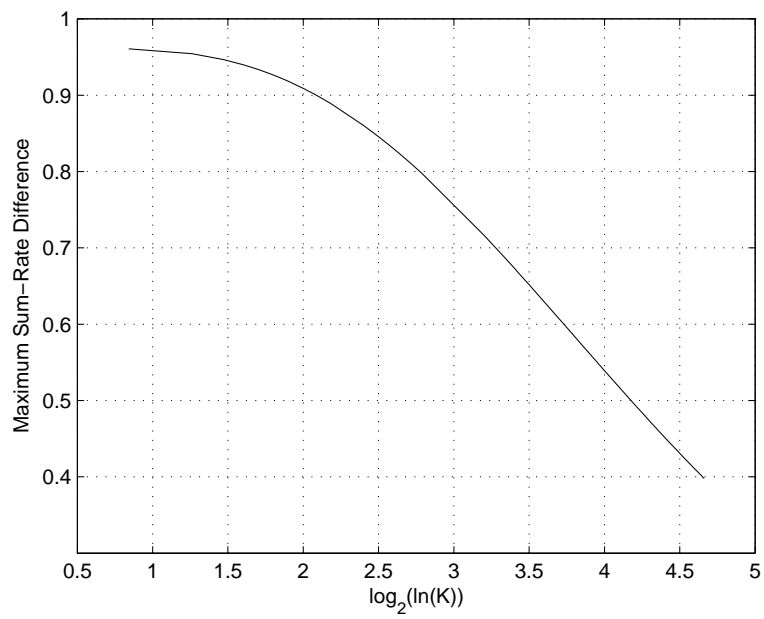


Fig. 8. Maximum sum-rate difference between MMSE and MRC vs. $\log \ln K$ for $N_t = N_r = 4$ and $\rho = 3$ dB using the opportunistic scheduler with SINR feedback.